



Heterogeneous reactions of NO_2 with $\text{CaCO}_3\text{-(NH}_4)_2\text{SO}_4$ mixtures at different relative humidities

Fang Tan, Shengrui Tong, Bo Jing, Siqi Hou, Qifan Liu, Kun Li, Ying Zhang, and Maofa Ge

Beijing National Laboratory for Molecular Sciences (BNLMS), State Key Laboratory for Structural Chemistry of Unstable and Stable Species, Institute of Chemistry, Chinese Academy of Sciences, 100190, Beijing, China

5 Correspondence to Maofa Ge (gemaofa@iccas.ac.cn) and Shengrui Tong (tongsr@iccas.ac.cn)



Abstract

In this work, the heterogeneous reactions of NO_2 with $\text{CaCO}_3\text{-(NH}_4)_2\text{SO}_4$ mixtures with a series of weight percentage (wt%) of $(\text{NH}_4)_2\text{SO}_4$ were investigated using a diffuse reflectance infrared Fourier transform spectroscopy (DRIFTS) at different relative humidity (RH) values.

5 For comparison, the heterogeneous reactions of NO_2 with pure CaCO_3 particles and pure $(\text{NH}_4)_2\text{SO}_4$ particles, as well as the reaction of CaCO_3 with $(\text{NH}_4)_2\text{SO}_4$ particles were also studied. The results indicated that NO_2 did not show any significant uptake on $(\text{NH}_4)_2\text{SO}_4$ particles, and it reacted with CaCO_3 particles to form calcium nitrate under both dry and wet conditions. The heterogeneous reactions of NO_2 with $\text{CaCO}_3\text{-(NH}_4)_2\text{SO}_4$ mixtures were

10 markedly dependent on RH. Calcium nitrate was formed from the heterogeneous reactions at all the RHs investigated, whereas $\text{CaSO}_4 \cdot 0.5\text{H}_2\text{O}$ (bassanite), $\text{CaSO}_4 \cdot 2\text{H}_2\text{O}$ (gypsum) and $(\text{NH}_4)_2\text{Ca}(\text{SO}_4)_2 \cdot \text{H}_2\text{O}$ (koktaite) were produced depending on RH. Under dry condition, the NO_3^- mass concentrations for the $\text{CaCO}_3\text{-(NH}_4)_2\text{SO}_4$ mixtures had a negative linear relation with the mass fraction of $(\text{NH}_4)_2\text{SO}_4$ in the mixtures. In this condition, the heterogeneous

15 uptake of NO_2 on the mixtures was similar to that on CaCO_3 particles. Under wet conditions, the $\text{CaCO}_3\text{-(NH}_4)_2\text{SO}_4$ mixtures exhibited a promotive effect on the heterogeneous uptake of NO_2 and the formation of nitrate, especially at medium RHs. In addition, the heterogeneous uptake of NO_2 on the mixtures of CaCO_3 and $(\text{NH}_4)_2\text{SO}_4$ was found to favor the formation of bassanite and gypsum due to the decomposition of CaCO_3 and the coagulation of Ca^{2+} and

20 SO_4^{2-} . A possible reaction mechanism was proposed and atmospheric implications were discussed.



1. Introduction

Haze with high level of fine particulate matter with diameters less than 2.5 μm ($\text{PM}_{2.5}$) occurs frequently in China in recent years (Fang et al., 2009; Kulmala, 2015). Emissions of gases pollutants, e.g., SO_2 , NO_x , NH_3 , and volatile organic compounds (VOCs), result in a series of atmospheric chemical reactions, which are responsible for the formation of secondary particles and the occurrence of haze (Zhang et al., 2015; Wang et al., 2013; Guo et al., 2014). Chemical analyses show that sulfate, nitrate, and ammonium are the major aerosol constituents of $\text{PM}_{2.5}$ (Yang et al., 2011; Huang et al., 2014). Pathak et al. (2009) discovered that nitrate concentration showed a correlation with sulfate concentration as well as the RH value in ammonium-poor areas. Kong et al. (2014a) found strong negative correlation between the mass fraction of nitrate and that of sulfate in acidic atmospheric particles during air pollution episodes. Although atmospheric particulate sulfate, nitrate, and ammonium were found to be correlated by numerous field measurements in different locations (Sullivan et al., 2007; Quan et al., 2008; Duan et al., 2003; Possanzini et al., 1999; Querol et al., 1998), there is still a lack of knowledge to explain the significant relevance.

Mineral dust is a major fraction of airborne particulate matter on a global scale (Tegen et al., 1996) with an estimated annual emission of 1000-3000 Tg of solids into the troposphere (Li et al., 1996). Mineral aerosols provide significant reactants and reactive sites for atmospheric heterogeneous reactions (Usher et al., 2003). Modeling studies indicated that mineral aerosols was highly associated with nitrate formation in the atmosphere (Dentener et al., 1996). Calcium carbonate represents an important and reactive mineral dust component, approximately accounting for 20-30% of the total dust loading (Usher et al., 2003; Li et al., 2006; Al-Hosney and Grassian, 2005; Prince et al., 2007). Calcium carbonate particle is converted to calcium nitrate after exposing to nitrogen oxides and HNO_3 in the atmosphere (Li et al., 2009; Laskin et al., 2005). Field measurements reveal that mineral dust particles are often mixed with ammonium sulfate aerosols through coagulation during long-range transport (Levin et al., 1996; Zhang et al., 2000). Korhonen et al. (2003) suggested that ammonium sulfate coating of mineral dust by heterogeneous nucleation of H_2SO_4 , NH_3 , and H_2O could occur at atmospheric sulphuric acid concentration. Additionally, Mori et al. (1998) have



found the coagulation between CaCO_3 and $(\text{NH}_4)_2\text{SO}_4$ could form kokaite and gypsum, attributing to the interaction of ions under humid condition. Ma et al. (2013) also discovered that mixed CaCO_3 - $(\text{NH}_4)_2\text{SO}_4$ particles had synergistic effects on the formation of gypsum in the humidifying-dehumidifying processes.

5 A few studies have shown that coexisting components play a role in the heterogeneous uptake of trace gases on atmospheric particles. Kong et al. (2014b) found that coexisting nitrate could significantly accelerate the formation rate of sulfate on hematite surface, resulting in surface-adsorbed HNO_3 , gas-phase N_2O and HONO productions. Zhao et al. (2013) found that coexisting surface nitrate had different effects on the uptake of H_2O_2 on
10 mineral particle surfaces depending on RH. The catalysis and basic coexists could increase the formation of sulfate on NaCl particle surfaces (Li et al., 2007). To the best of our knowledge, the heterogeneous reaction of atmospheric trace gases on mixed CaCO_3 - $(\text{NH}_4)_2\text{SO}_4$ particles has not been reported.

Furthermore, an increase in tropospheric NO_2 concentration has been observed in recent
15 years across many developing regions due to fossil fuel combustion and biomass burning (Zhang et al., 2007; Sheel et al., 2010; Ghude et al., 2009; Shi et al., 2008; Richter et al., 2005; Irie et al., 2005). Atmospheric NO_2 concentration ranges from 70 part per billion (ppb) during photochemical smog events to 100-500 ppb in polluted urban environment (Huang et al., 2015; Zamaraev et al., 1994). NO_2 is one such critical anthropogenic gaseous pollutant,
20 which reduces air quality and affects global tropospheric chemistry. NO_2 plays a crucial role in the photochemical induced catalytic production of ozone, leading to photochemical smog and increasing tropospheric ozone concentration (Volz and Kley, 1988). Moreover, the heterogeneous reactions of NO_2 can also lead to the deposition of nitric acid, as well as the formation of gas phase HONO (Jaegle et al., 1998; Brimblecombe and Stedman, 1982;
25 Goodman, 1999). Furthermore, the heterogeneous uptake of NO_2 on mineral aerosols was responsible for the nitrate accumulation in dust events (Usher et al., 2003). A number of laboratory studies investigated the heterogeneous reaction of NO_2 with mineral dust (Underwood et al. 1999b; Borensen et al., 2000; Finlayson-Pitts et al., 2003; Liu et al., 2015; Guan et al., 2014). Miller and Grassian (1998) discovered that NO_2 reacted with Al_2O_3 and



TiO₂ particles to form surface nitrite and nitrate. Underwood et al. (1999a) measured the uptake coefficients of NO₂ on Al₂O₃, TiO₂, and Fe₂O₃ particles using a Knudsen cell. Li et al. (2010) determined the Brunauer-Emmett-Teller (BET) area-corrected initial uptake coefficients to be 10⁻⁹ and 10⁻⁸ for the heterogeneous uptake of NO₂ on CaCO₃ particles under
5 dry and wet conditions, respectively. However, there are big gaps between the results of modeling studies and field measurements about the quantities and accumulation of nitrate, especially in haze periods (Zheng et al., 2015).

In the present study, the heterogeneous reactions of NO₂ with the mixtures of CaCO₃ and (NH₄)₂SO₄, pure CaCO₃ particles, and pure (NH₄)₂SO₄ particles at different RHs were
10 investigated using a DRIFTS reactor. The surface adsorbed products were monitored and the uptake coefficients of NO₂ were determined. The aim of this work is to explore the kinetics and mechanism of the heterogeneous reactions of NO₂ with CaCO₃-(NH₄)₂SO₄ mixtures and its relevance to RH. The results are helpful for further exploring the correlations among particulate nitrate, sulfate, and ammonium concentration in the atmosphere and partly
15 contribute to understanding of multicomponent reaction systems in practical environment system.

2. Experimental

CaCO₃ (99.5 %) and (NH₄)₂SO₄ (99.9%) were purchased from Alfa Aesar. CaCO₃ and (NH₄)₂SO₄ were mechanically mixed and grinded together in order to obtain uniform
20 mixtures with the mass percentage of (NH₄)₂SO₄ in the mixtures ranged from 10% to 93% (wt%) (which were denoted as FAS-10, FAS-20, FAS-40, FAS-57, FAS-75, FAS-87, and FAS-93, respectively). The BET surface areas of pure CaCO₃ and (NH₄)₂SO₄ particles were determined to be 8.15 and 0.19 m² g⁻¹, respectively, (Autosorb-1-MP automatic equipment (Quanta Chrome Instrument Co.)). The BET area of the mixtures were determined to be 8.06,
25 6.62, 4.54, 3.21, 2.34, 1.67, and 0.89 m² g⁻¹ corresponding to the mixtures mentioned above. NO₂ (0.1%, Beijing Huayuan Gas Chemical Industry Co., Ltd.) and N₂ (>99.999%, Beijing Tailong Electronics Co., Ltd.) were used in this study.

In the gas supply system, N₂ was split into two streams; one was dehumidified by silica gel



and molecular sieve to insure RH less than 1% which was called dry condition, the other one was humidified by bubbling through ultrapure water. The flux of dry N₂, humid N₂, and NO₂ were adjusted to reach expected RH (<1%, 40%, 60%, and 85% RH) conditions with the total flow of 400 sccm, using mass flow controllers (Beijing Sevenstar electronics Co., LTD).

5 Concentration of NO₂ entering reactor was diluted to 2.6×10^{15} molecules cm⁻³ by mixing with N₂. RH and temperature of the inflow of sample cell were measured using a commercial humidity and temperature sensor (HMT330; Vaisala) with a measurement accuracy of $\pm 1\%$ RH and $\pm 0.2^\circ\text{C}$, respectively.

In situ DRIFTS experiment was used to monitor reactions in real time without interrupting the reaction processes and provide mechanistic details and kinetic data (Vogt and Finlaysonpitts, 1994). Infrared spectra of sample surfaces were recorded with a Nicolet FTIR Spectrometer 6700, which was equipped with a liquid-nitrogen-cooled narrow band mercury-cadmium-telluride (MCT) detector and DRIFTS optics (Model CHC-CHA-3, Harrick Scientific Corp.). The DRIFTS equipment has been described elsewhere (Tong et al.,

15 2010). The spectra were measured at a resolution of 4 cm^{-1} in the spectral range from 4000 to 650 cm^{-1} . Each spectrum was generally averaged from 100 scans with a time resolution of 40 s. In situ DRIFTS experiments were carried out on CaCO₃-(NH₄)₂SO₄ mixtures, CaCO₃ particles, and (NH₄)₂SO₄ particles, respectively. About 30 mg samples were placed into the stainless steel sample holder (10 mm diameter, 0.5 mm depth). The investigated samples were

20 exposed to pure nitrogen with expected RH for 20 minutes to establish adsorption equilibrium. Then infrared spectra of the unreacted powder samples were collected as background so that reaction products were observed as positive adsorption bands while losses of surface species as negative adsorption bands. Subsequently, NO₂ was introduced into the reaction chamber at a stable RH for 120 min. All the spectra were automatically collected

25 through a Series program in OMNIC software.

The products formed on the samples after reaction with NO₂ were analyzed by ion chromatography. The filtered solution was analyzed by using a Dionex ICS 900system, equipped with a Dionex AS 14A analytical column and a conductivity detector (DS5). The reacted samples were sonicated for 20 min in 8 ml ultrapure water.



3. Results and discussion

3.1 Surface products characterization

Figure 1 represents the IR spectra of surface products when the samples were exposed to NO₂ for 120 min at different RHs. Under dry condition (Fig. 1a), absorption bands centered at 746, 816, 1040, 1300, and 1330 cm⁻¹ which were assigned to surface nitrate could be observed on CaCO₃ particle surfaces (FAS-0) and the mixtures (Goodman et al., 2001; Goodman et al., 2000; Al-Hosney and Grassian, 2005). Moreover, peaks at 1630 and 3540 cm⁻¹ were assigned to crystal hydrate water in calcium nitrate (Li et al., 2010). It suggested that calcium nitrate was formed on CaCO₃ particle surfaces and the mixtures of CaCO₃ and (NH₄)₂SO₄. The detailed vibrational assignments were listed in Table 1. Two peaks observed at 1689 and 838 cm⁻¹ could be attributed to the $\nu(\text{C}=\text{O})$ and $\delta_{\text{oop}}(\text{CO}_3)$ of adsorbed carbonic acid, respectively, indicating that carbonic acid acted as an intermediate production under dry condition (Al-Hosney, 2004; Al-Abadleh et al., 2004). Besides, adsorbed nitric acid was also formed with peaks centered at 1710 and 1670 cm⁻¹, which were assigned to the asymmetric stretching of adsorbed nitric acid (Goodman, 1999). At the same time, negative bands ranging from 2800 to 3400 cm⁻¹ could be ascribed to the loss of surface adsorbed water and negative peaks at 3640 and 3690 cm⁻¹ were corresponding to the two types of hydroxyl ions on CaCO₃ particle surfaces (Kuriyavar et al., 2000). No obvious negative peaks could be observed when the samples exposed to dry pure nitrogen for 120 min which indicated that surface adsorbed water and hydroxyl ions participated in the reaction.

Compared with the spectrum of FAS-0, several additional weak absorptions appeared at 1008, 1096, 1155 cm⁻¹ on the CaCO₃-(NH₄)₂SO₄ mixtures, which could be attributed to the vibration modes of SO₄ tetrahedra in CaSO₄ 0.5H₂O (bassanite) (Prasad, 2005; Liu et al., 2009). The vibration modes of water group in bassanite were too weak to be observed. In addition, the peak at 1215 cm⁻¹ slightly grew in intensity during the whole heterogeneous reaction period of NO₂ with the mixtures, whereas it grew fast at the early stage of the reaction of NO₂ with CaCO₃ particles, and then diminished after reaching a maximum value



at about 30 min (see Fig. S1). This band described before was ascribed to nitrite species, which would convert to nitrate as the reaction proceeded (Miller and Grassian, 1998; G. M. Underwood, 1999b; Wu et al., 2013). To probe this product, samples after reaction with NO_2 for different times were detected by IC. The results showed that nitrite was increased during the first 30 min of the reaction of NO_2 with CaCO_3 particles, whereas it was too little to be detected after the reaction lasted 60 min. For the reaction of NO_2 with the mixtures, nitrite could be detected during the all process.

At 40% RH (Fig. 1b), the absorption bands of nitrate shifted from 1040 cm^{-1} to 1043 cm^{-1} , 746 cm^{-1} to 749 cm^{-1} , and 816 cm^{-1} to 828 cm^{-1} , respectively, compared to those under dry condition. Meanwhile, the shoulder peak at 1300 cm^{-1} belong to asymmetric stretching of nitrate became ambiguous. The frequency shifts of nitrate adsorption bands were caused by the phase transition of calcium nitrate. It was reported that calcium nitrate was in amorphous hydrates state at RH below 7% (Liu et al., 2008), and it deliquesced to form a saturated solution droplet at 18% RH (Tang and Fung, 1997). For the absorption bands of nitrate on the mixtures of CaCO_3 and $(\text{NH}_4)_2\text{SO}_4$, there was a new shoulder peak at 1365 cm^{-1} which were attributed to the $\nu_3(\text{NO}_3)$ in NH_4NO_3 (Schlenker et al., 2004). Moreover, the formation of $\text{CaSO}_4 \cdot 0.5\text{H}_2\text{O}$ was enhanced at 40% RH compared to that under dry condition, as features became apparent at 1155 , 1096 , and 1008 cm^{-1} , concomitant with the appearance of the peaks at 1620 , 3555 , and 3605 cm^{-1} due to the vibration modes of water group in bassanite (Prasad et al., 2005). Additionally, signatures at 1670 cm^{-1} , 1570 cm^{-1} on the samples suggested the formation of nitric acid, HCO_3^- during the heterogeneous reaction, respectively. And the signature at 1189 cm^{-1} (Schlenker et al., 2004) on the mixtures suggested that HSO_4^- was produced.

When RH reached 60% (Fig. 1c), water film was formed on particle surfaces with a band centered at 1650 cm^{-1} and a broad band composed of three peaks at 3260 , 3400 , and 3570 cm^{-1} , which could be assigned to the vibration modes of surface condensed water (Goodman et al., 2000). Meanwhile, the asymmetric stretching of surface nitrate appeared as a sharp peak at 1338 cm^{-1} . This was likely due to calcium nitrate incorporated into surface adsorbed water film and formed free aquated ions, based on the truth that only one sharp asymmetric



stretching peak existed for free aquated ions NO_3^- (Gatehouse et al., 1957). The absorptions bands due to NH_4NO_3 could also be observed at 1365 cm^{-1} for the mixtures of CaCO_3 and $(\text{NH}_4)_2\text{SO}_4$. Additionally, new peaks could be observed at 1168 , 1145 , and 1117 cm^{-1} , which were attributed to the $\nu_3(\text{SO}_4)$ mode of gypsum. The IR absorption bands of bassanite and gypsum were difficult to be distinguished in the region between 1000 and 1250 cm^{-1} since the $\nu_3(\text{SO}_4)$ mode of them had some overlaps in this region. gypsum showed two IR-active modes in the bending modes of crystal hydrate water at 1620 and 1685 cm^{-1} , while bassanite had only one band at 1620 cm^{-1} . And the two stretching modes of crystal hydrate water appeared at 3545 , and 3400 cm^{-1} for gypsum, at 3555 and 3610 cm^{-1} for bassanite (Prasad, 2005). Furthermore, it should be noticed that the peak at 3400 cm^{-1} from $\text{CaSO}_4 \cdot 2\text{H}_2\text{O}$ on the samples of FAS-40, FAS-57, FAS-75, and FAS-87 were much stronger than the peak at 3400 cm^{-1} from condensed water on CaCO_3 particles. Therefore it can be inferred that $\text{Ca}(\text{NO}_3)_2$, NH_4NO_3 , $\text{CaSO}_4 \cdot n\text{H}_2\text{O}$ (gypsum and bassanite) were produced at 60% RH from the heterogeneous reaction of NO_2 with the CaCO_3 - $(\text{NH}_4)_2\text{SO}_4$ mixtures.

The spectrum of FAS-0 in Fig. 1d was similar to that in Fig. 1c, while there were considerable changes for spectra of the mixtures as RH increased to 85%. Peaks observed at 981 , 998 , 1131 , 1177 cm^{-1} on the mixtures due to the stretching vibration modes of SO_4^{2-} as well as peaks at 2860 , 3064 , 3192 cm^{-1} assigned to the stretching vibration modes of NH_4^+ indicated the formation of $(\text{NH}_4)_2\text{Ca}(\text{SO}_4)_2 \cdot \text{H}_2\text{O}$ (koktaite) (Jentzsch et al., 2012). The absorption band of nitrate overlapped with that of koktaite at 749 cm^{-1} . It can be inferred that koktaite, an intermediate production of gypsum, was formed rapidly as a result of the interaction of ions in the liquid film after the deliquescence of surface salts (Cziczo et al., 1997; Lightstone et al., 2000). Additionally, the increasing intensity of absorption bands at 1570 cm^{-1} implied that the decomposition of CaCO_3 was enhanced at 85% RH.

In addition, it can be concluded from Fig. 1 that NO_2 did not show any significant uptake on pure $(\text{NH}_4)_2\text{SO}_4$ particles (FAS-100) at all the RHs investigated. The products formed from the heterogeneous reactions of NO_2 with the CaCO_3 - $(\text{NH}_4)_2\text{SO}_4$ mixtures were strongly dependent on RH. $\text{Ca}(\text{NO}_3)_2$ and bassanite were produced under both dry and wet conditions, gypsum and koktaite were formed at 60% and 85% RH.



In another set of experiments, the mixture of FAS-57 was exposed to nitrogen with corresponding RHs to investigate the solid-state reaction of CaCO_3 with $(\text{NH}_4)_2\text{SO}_4$ without the introduction of NO_2 . As shown in Fig. 2, no new absorption bands occurred after exposing to dry nitrogen for 120 min. The weak peak at 1189 cm^{-1} due to HSO_4^- appeared as a main adsorption peak and no obvious absorption band due to bassanite could be observed on the mixture of FAS-57 at 40% RH. The results suggested that little reaction occurred between CaCO_3 and $(\text{NH}_4)_2\text{SO}_4$ particles under dry condition and 40% RH, therefore the heterogeneous reactions of NO_2 with the CaCO_3 - $(\text{NH}_4)_2\text{SO}_4$ mixtures were responsible for the formation of bassanite. Furthermore, absorption bands attributed to bassanite, gypsum, kokaite, and HSO_4^- could be observed on the sample of FAS-57 after exposed to nitrogen at 60% and 85% RH. It was in good agreement with the results reported by Mori et al. (1998) that gypsum was formed from the chemical reaction between $(\text{NH}_4)_2\text{SO}_4$ and CaCO_3 with kokaite acting as an intermediate product. The integrated absorbance of band between 1100 and 1250 cm^{-1} for the sample of FAS-57 at 60% and 85% RH in Fig. 2 was about fifty percent and seventy percent of that for FAS-57 at corresponding RH in Fig. 1. It indicated that the mixtures of CaCO_3 and $(\text{NH}_4)_2\text{SO}_4$ undergo obvious reaction at 60% and 85% RH without the introduction of NO_2 . And there were additional gypsum and kokaite products formed from the heterogeneous reaction of NO_2 with the mixtures in comparison with the reaction between CaCO_3 and $(\text{NH}_4)_2\text{SO}_4$ particles under 60% and 85% RH.

3.2 Uptake coefficients and kinetics

The formation rates of nitrate on CaCO_3 particles and the mixtures were studied. The nitrate formed during the reaction was presented by the integrated absorbance (I_A) of the IR peak area between 1390 and 1250 cm^{-1} . The peak at 1043 cm^{-1} was not used to avoid the interruption of the absorptions of sulfates. Figure 3 represents the integrated absorbance of nitrate as a function of time at different RHs. The nitrate formation rates were fast at initial stage, and then slowed down after a transition stage under dry condition. Moreover, the lasting time of initial stage was shortened with increasing mass fraction of $(\text{NH}_4)_2\text{SO}_4$, e.g., it lasted about 80 min for pure CaCO_3 particles, 20 min for the mixture of FAS-75 and 5 min for the mixture of FAS-93. The possible reasons were that active sites decreased with



increasing $(\text{NH}_4)_2\text{SO}_4$ content and the reactions occurred only on the surfaces under dry condition. While the lasting time of initial stage was extended with increasing RH, e.g., it extended to 80 min for the mixture of FAS-75, to 50 min for the mixture of FAS-93, and even longer than 120 min for the mixtures with mass fraction of $(\text{NH}_4)_2\text{SO}_4$ smaller than 57% at 40% RH. The boundaries between initial stage and transition stage became ambiguous at 60% RH and finally disappeared at 85% RH for all the CaCO_3 - $(\text{NH}_4)_2\text{SO}_4$ mixtures, implying that the reactions were not limited to the surface under wet conditions.

The integrated absorbance (I_A) for nitrate ions on the samples had a linear relationship with the amount of nitrate determined by ion chromatography $\{\text{NO}_3^-\}$:

$$\text{The nitrate ions: } \{\text{NO}_3^-\} = (\text{integrated absorbance } I_A) \times f \quad (1)$$

Here f is conversion factor. It is calculated to be $(2.11 \pm 0.17) \times 10^{17}$ ions/int.abs at 85% RH and $(3.35 \pm 0.13) \times 10^{17}$ ions/int.abs at 60%, 40% RH and dry condition (see Fig. S2). The conversion factor f may change with the chemical environment of surface nitrate which is related to surface condensed water and ion interaction (Li et al., 2010). Then nitrate formation rates $d\{\text{NO}_3^-\}/dt$ can be calculated from f and the slope of integrated absorbance as a function of time.

As shown in Fig. 4, the initial nitrate formation rate for the samples showed a maximum value under dry condition, whereas the stable formation rates were much slower in this condition. The initial nitrate formation rates increased as RH increased from 40% RH to 60% and 85% RH for the uptake of NO_2 on CaCO_3 particle surfaces. For the mixtures with mass fraction of $(\text{NH}_4)_2\text{SO}_4$ larger than 57%, it showed an opposite variation that initial nitrate formation rates at 40% RH were higher than that at 60% RH, followed by that at 85% RH. Besides, nitrate formation rates decreased more evidently with increasing $(\text{NH}_4)_2\text{SO}_4$ content at 85% RH and dry condition than at 40% and 60% RH, e.g., the initial nitrate formation rates for the mixture of FAS-93 under dry condition, 40%, 60%, and 85% RH were 47%, 70%, 62%, and 34% of that for CaCO_3 particles at corresponding RH, respectively. It could also be demonstrated by the result that initial nitrate formation rates for CaCO_3 particles at 40%, 60%, and 85% RH were 64%, 67%, and 72% of that under dry condition, respectively. For the



mixture of FAS-93, the initial nitrate formation rates at 40%, 60%, and 85% RH were 95%, 87%, and 60% of that under dry condition. Similar results could be concluded from the initial nitrate formation rates of other $\text{CaCO}_3\text{-(NH}_4)_2\text{SO}_4$ mixtures. In summary, the initial nitrate formation rates of the reaction of NO_2 with $\text{CaCO}_3\text{-(NH}_4)_2\text{SO}_4$ mixtures were accelerated to some degree at 40% and 60% RH in comparison with the reaction of NO_2 with pure CaCO_3 particles, whereas it was inhibited slightly at 85% RH.

The reactive uptake coefficient (γ) is defined as the rate of the reactive collisions with the surface divided by the total number of surface collisions per unit time (Z).

$$\gamma = \frac{dN(\text{NO}_2)/dt}{Z} \quad (2)$$

$$Z = \frac{1}{4} A_s [\text{NO}_2] \sqrt{\frac{8RT}{\pi M_{\text{NO}_2}}} \quad (3)$$

Where $N(\text{NO}_2)$ is the number of reactive NO_2 collisions with the surface, A_s is the effective surface area of samples and $[\text{NO}_2]$ is the gas-phase concentration of NO_2 . R represents the gas constant, T represents the temperature and M_{NO_2} is the molecular weight of NO_2 . The rate of reactive collision can be obtained from the nitrate formation rate $d\{\text{NO}_3^-\}/dt$, then the reactive uptake coefficient can be calculated by:

$$\gamma = \frac{d\{\text{NO}_3^-\}/dt}{Z} \quad (4)$$

The uptake coefficients of NO_2 on CaCO_3 particles and $\text{CaCO}_3\text{-(NH}_4)_2\text{SO}_4$ mixtures were calculated using both BET and geometric surface area, which could be considered as two extreme cases (Ullerstam et al., 2002). The results are listed in Table 2. The initial uptake coefficients corresponding to BET surface area for NO_2 on CaCO_3 particle surfaces are $(3.34 \pm 0.14) \times 10^{-9}$, $(2.04 \pm 0.07) \times 10^{-9}$, $(2.23 \pm 0.22) \times 10^{-9}$, and $(2.28 \pm 0.17) \times 10^{-9}$ for dry condition, 40%, 60%, and 85% RH, respectively, well consistent with the previous measurement results (Li et al., 2010; Brönsen et al., 2000). The γ_{BET} is approximately a factor of 10^4 smaller than the $\gamma_{\text{geometric}}$. The γ_{BET} for the uptake of NO_2 on the mixtures was enhanced with increasing $(\text{NH}_4)_2\text{SO}_4$ content because of the decrease of BET surface area. On the contrary, the $\gamma_{\text{geometric}}$



decreased with increasing $(\text{NH}_4)_2\text{SO}_4$ content due to the decrease of nitrate formation rate.

The mass concentrations of NO_3^- formed on the samples after reaction with NO_2 were detected by IC, as shown in Fig. 5. The NO_3^- mass concentrations for CaCO_3 particles are 3.22 ± 0.17 , 3.31 ± 0.03 , 3.38 ± 0.35 , and 3.47 ± 0.32 mg/g under dry condition, 40%, 60% and 85% RH, respectively. It suggests that the NO_3^- mass concentration increase slightly with higher RH for pure CaCO_3 particles. For the CaCO_3 - $(\text{NH}_4)_2\text{SO}_4$ mixtures, the NO_3^- mass concentrations under dry condition are obviously smaller than those at 85% RH, and it exhibits maximum values at 40% or 60% RH. The results indicate that CaCO_3 - $(\text{NH}_4)_2\text{SO}_4$ mixtures have a different tendency with RH compared to pure CaCO_3 particles. In addition, it should be noticed that the NO_3^- mass concentrations has a negative linear relation with $(\text{NH}_4)_2\text{SO}_4$ mass fraction in the mixtures under dry condition, the R^2 of liner fit is 0.993. Based on the product analysis, the reaction of NO_2 with CaCO_3 - $(\text{NH}_4)_2\text{SO}_4$ mixtures is very similar to the reaction of NO_2 with pure CaCO_3 particles under dry condition, which indicates that the $(\text{NH}_4)_2\text{SO}_4$ has little effects on the formation of NO_3^- in this condition. Moreover, the concentrations of NO_3^- of the mixtures under wet conditions are markedly larger than those under dry condition. The nitrate concentrations for the mixtures of FAS-10 and FAS-20 at 40% and 60% RH are even larger than that for pure CaCO_3 particles. The NO_3^- mass concentrations for the mixture of FAS-57 are 3.23 ± 0.09 , 3.09 ± 0.14 , 2.42 ± 0.07 mg/g at 40%, 60% and 85% RH, respectively, which are increased by a factor of 2.1, 2.0, and 1.6 in comparison with the NO_3^- mass concentrations for FAS-57 under dry condition (1.55 ± 0.08 mg/g). Similar results can be concluded from the NO_3^- mass concentrations for other mixtures. Moreover, no obvious NO_3^- is formed on pure $(\text{NH}_4)_2\text{SO}_4$ particles under all conditions investigated. These results clearly reveal that the mixtures exhibit a promotive effect on the heterogeneous uptake of NO_2 to form nitrate compared to CaCO_3 particles under wet conditions.

The results described above indicate that relative humidity plays a vital role in the heterogeneous reaction of NO_2 with CaCO_3 - $(\text{NH}_4)_2\text{SO}_4$ mixtures. Under dry condition, little reaction occurs between CaCO_3 and $(\text{NH}_4)_2\text{SO}_4$ with the absence of water vapor. Therefore, nitrate formed on the mixtures under dry condition is mainly produced from the

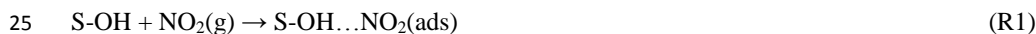


heterogeneous uptake of NO_2 on CaCO_3 particles without the participation of $(\text{NH}_4)_2\text{SO}_4$. At 40% RH, the solid-state reaction between CaCO_3 and $(\text{NH}_4)_2\text{SO}_4$ particles can be neglected, implying that solid-state reaction has little effects on the heterogeneous reaction. Meanwhile, the deliquesced $\text{Ca}(\text{NO}_3)_2$ could interact with $(\text{NH}_4)_2\text{SO}_4$ particles to form microcrystallites of NH_4NO_3 and $\text{CaSO}_4 \cdot n\text{H}_2\text{O}$, which may improve the ionic mobility of the surface ions (Allen et al., 1996), modify the surface structure and expose additional active sites on CaCO_3 particles in the mixtures (Al-Hosney and Grassian, 2005). However, the nitrate formation rates and nitrate concentrations at 60% RH was decreased compared to those at 40% RH for the mixtures with mass percentage of $(\text{NH}_4)_2\text{SO}_4$ larger than 57%. At 60% RH, water film on particle surfaces promotes the reaction between CaCO_3 and $(\text{NH}_4)_2\text{SO}_4$, leading to the formation of $\text{CaSO}_4 \cdot n\text{H}_2\text{O}$. In this condition, CaCO_3 particles are partly consumed during the solid-state reaction process. And $\text{CaSO}_4 \cdot n\text{H}_2\text{O}$ adhering on CaCO_3 particle surfaces may block active sites and inhibit the heterogeneous reaction. Consequently, the solid state reaction between CaCO_3 and $(\text{NH}_4)_2\text{SO}_4$ particles exhibits an inhibiting effect on the uptake of NO_2 and the formation of nitrate. As for 85% RH, the deliquescence of $(\text{NH}_4)_2\text{SO}_4$ and surface nitrate leads to more water uptake on the mixture surfaces. The coagulation of ions in water film facilitates the formation of kokaite and $\text{CaSO}_4 \cdot n\text{H}_2\text{O}$. Thus, nitrate formation rate and nitrate concentration decrease at 85% RH.

3.3 Mechanism

According to the experimental observations described above, a reaction mechanism for the heterogeneous reactions of NO_2 with CaCO_3 - $(\text{NH}_4)_2\text{SO}_4$ mixtures was proposed.

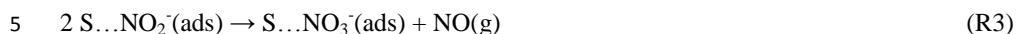
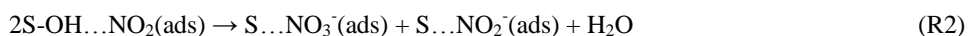
Gas phase NO_2 attached to surface OH groups on CaCO_3 particle surfaces, as shown in (R1), where (g) is the gas phase and (ads) is the adsorbed phase.



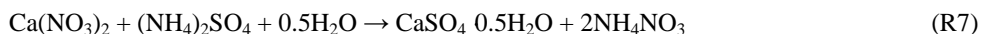
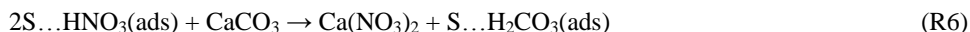
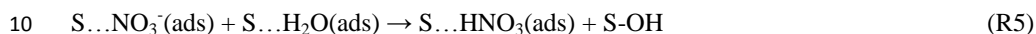
Börensén et al. (2000) proposed that two adsorbed-phase NO_2 molecules result in surface nitrate and nitrite products through a disproportionation reaction. Underwood et al. (1999b)



suggested that NO_2 (g) reacted to form adsorbed nitrite species initially and then react with another surface nitrite or with gas-phase NO_2 to form nitrate. Nitrite was detected by FTIR and IC in this study. The reaction process can be described as:



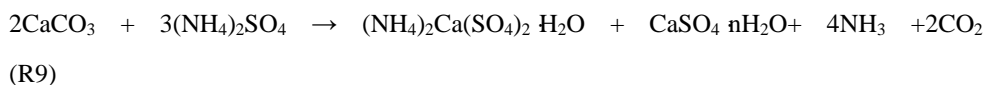
Under dry condition, the surface nitrate was in equilibrium with surface adsorbed water and adsorbed HNO_3 species (R5). Adsorbed H_2CO_3 can exist on CaCO_3 particle surfaces (R6) and there was weak chemical interaction between $\text{Ca}(\text{NO}_3)_2$ and $(\text{NH}_4)_2\text{SO}_4$ (R7).



At 40% RH, $\text{Ca}(\text{NO}_3)_2$ deliquesced to form a saturated solution droplet and reacted with $(\text{NH}_4)_2\text{SO}_4$:



At 60% RH, the interaction between CaCO_3 and $(\text{NH}_4)_2\text{SO}_4$ in the presence of surface adsorbed water film can be expressed as R9:



20 It should be noticed that NH_3 was detected by PTR-MS (Proton-transfer-reaction mass spectrometry) under wet conditions in this study. NH_3 can also be released from the decomposition of NH_4NO_3 (R10).



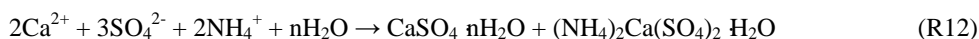
At the same time, the heterogeneous reaction of NO_2 with surface adsorbed water has been
 25 demonstrated to form adsorbed $\text{HNO}_3(\text{ads})$ and gaseous $\text{HONO}(\text{g})$ (Svensson et al., 1987;



Jenkin et al., 1988; Goodman et al., 1999).



At 85% RH, the interaction of ions in the water film can be expressed as:



5

4. Conclusions and atmospheric implications

The surface products and kinetics of the heterogeneous reactions of NO_2 with pure CaCO_3 particles, pure $(\text{NH}_4)_2\text{SO}_4$ particles, and CaCO_3 -(NH_4) $_2\text{SO}_4$ mixtures were investigated under various RHs, using DRIFTS technique. And the solid-state reaction between CaCO_3 and
 10 $(\text{NH}_4)_2\text{SO}_4$ particles were studied for comparison. All these reactions can occur in practical atmospheric conditions, which can be expressed in Fig. 6. The findings in this study have important atmospheric implications.

Calcium nitrate was produced from the heterogeneous reaction of NO_2 with CaCO_3 -(NH_4) $_2\text{SO}_4$ mixtures under both dry and wet conditions, and bassanite, gypsum and
 15 koktaite were formed depending on RH. It suggested that chemical composition in particulate phase was changed during the heterogeneous process, which can affect the physicochemical characteristics of atmospheric particles, including hygroscopicity, optical properties, and chemical reactivity. Besides, koktaite was detected in aerosols collected in Beijing, while it was absent in the soil where the Asian dust originates (Mori et al., 2003), large uncertainties
 20 remain about its formation in the atmosphere. The results presented here provide evidence that the heterogeneous reactions of mixed CaCO_3 -(NH_4) $_2\text{SO}_4$ particles with atmospheric acid trace gases was a possible source of koktaite. Also, the results indicated that the uptake of NO_2 and the formation of nitrate promoted removing SO_4^{2-} from water soluble species such as $(\text{NH}_4)_2\text{SO}_4$ to insoluble gypsum species, which could reduce the atmospheric water soluble
 25 sulfate content.

Gas phase products such as NH_3 could be released during the heterogeneous reaction of NO_2 with CaCO_3 -(NH_4) $_2\text{SO}_4$ mixtures. In the atmosphere NH_3 is mainly emitted from



agriculture activities (such as fertilization and animal feeding) and biomass burning, and it plays an important role in nucleation and the growth of ion cluster and nanoparticles. The results in this study suggest that heterogeneous uptake of NO_2 on CaCO_3 particles with the presence of $(\text{NH}_4)_2\text{SO}_4$ may be a potential pathway for the transformation of NH_3 from particulate phase to gas phase.

Furthermore, the uptake-coefficients of NO_2 on CaCO_3 - $(\text{NH}_4)_2\text{SO}_4$ mixtures were determined, providing kinetic data for modeling studies. The results illustrate that the presence of $(\text{NH}_4)_2\text{SO}_4$ exhibits a promotive effect on the nitrate formation under wet conditions as a result of the interaction between $\text{Ca}(\text{NO}_3)_2$ and $(\text{NH}_4)_2\text{SO}_4$. On the contrary, the reaction between CaCO_3 and $(\text{NH}_4)_2\text{SO}_4$ particles has an inhibiting effect on the formation of nitrate during the heterogeneous reaction process, especially at high RH. Considering the abundance of $(\text{NH}_4)_2\text{SO}_4$ in the atmospheric aerosols, its mixtures with mineral dust may significantly affect nitrate formation and the content of nitrate in atmospheric particles. The multicomponent reaction systems under ambient RH conditions play as yet unclear but potentially vital role in atmospheric processes. To better understand the role of heterogeneous reactions in the atmospheric chemistry, the effects of ambient RH as well as multicomponent reaction systems should be considered.

The Supplement related to this article is available online.

Author contributions. Fang Tan and Shengrui Tong contribute equally to this work.

Acknowledgements. This project was supported by the Strategic Priority Research Program (B) of the Chinese Academy of Sciences (Grant No. XDB05010400), and the National Natural Science Foundation of China (Contract No.41475114, 91544227, 21477134).

References

- Al-Abadleh, H. A., Al-Hosney, H. A., and Grassian, V. H.: Oxide and carbonate surfaces as environmental interfaces: the importance of water in surface composition and surface reactivity, *J. Mol. Catal. A: Chem.*, 228, 47-54, doi:10.1016/j.molcata.2004.09.059, 2004.
- Al-Hosney, H. A., and Grassian, V. H.: Water, sulfur dioxide and nitric acid adsorption on



- calcium carbonate: A transmission and ATR-FTIR study, *Phys. Chem. Chem. Phys.*, 7, 1266-1276, doi:10.1039/b417872f, 2005.
- Al-Hosney, H. A., and Grassian, V. H.: Carbonic Acid: an important intermediate in the surface chemistry of calcium carbonate, *J. Am. Chem. Soc.*, 126, 8068-8069, 5 doi:10.1021/ja0490774, 2004.
- Allen, H. C., Laux, J. M., Vogt, R., Finlayson-Pitts, B. J., and Hemminger, J. C.: Water-induced reorganization of ultrathin nitrate films on NaCl: Implications for the tropospheric chemistry of sea salt particles, *J. Phys. Chem.*, 100, 6371-6375, doi:10.1021/jp953675a, 1996.
- 10 Börensen, C., Kirchner, U., Scheer, V., Vogt, R., and Zellner, R.: Mechanism and kinetics of the reactions of NO₂ or HNO₃ with alumina as a mineral dust model compound, *J. Phys. Chem. A*, 104, 5036-5045, doi:10.1021/jp994170d, 2000.
- Brimblecombe, P., and Stedman, D. H.: Historical evidence for a dramatic increase in the nitrate component of acid-rain, *Nature*, 298, 460-462, doi:10.1038/298460a0, 1982.
- 15 Cziczo, D. J., Nowak, J. B., Hu, J. H., and Abbatt, J. P. D.: Infrared spectroscopy of model tropospheric aerosols as a function of relative humidity: Observation of deliquescence and crystallization, *J. Geophys. Res.-Atmos.*, 102, 18843-18850, doi:10.1029/97jd01361, 1997.
- Dentener, F. J., Carmichael, G. R., Zhang, Y., Lelieveld, J., and Crutzen, P. J.: Role of mineral aerosol as a reactive surface in the global troposphere, *J. Geophys. Res.-Atmos.*, 101, 20 22869-22889, doi:10.1029/96jd01818, 1996.
- Duan, F. K., Liu, X. D., He, K. B., Lu, Y. Q., and Wang, L.: Atmospheric aerosol concentration level and chemical characteristics of water-soluble ionic species in wintertime in Beijing, China, *J. Environ. Monit.*, 5, 569-573, doi:10.1039/b303691j, 2003.
- Fang, M., Chan, C. K., and Yao, X.: Managing air quality in a rapidly developing nation: 25 China, *Atmos. Environ.*, 43, 79-86, doi:10.1016/j.atmosenv.2008.09.064, 2009.
- Finlayson-Pitts, B. J., Wingen, L. M., Sumner, A. L., Syomin, D., and Ramazan, K. A.: The heterogeneous hydrolysis of NO₂ in laboratory systems and in outdoor and indoor atmospheres: An integrated mechanism, *Phys. Chem. Chem. Phys.*, 5, 223-242, doi:10.1039/b208564j, 2003.



- Gatehouse, B. M., Livingstone, S. E., and Nyholm, R. S.: Infrared spectra of some nitrate-co-ordination complexes, *J. Chem. Soc., OCT*, 4222-4225, doi:10.1039/jr9570004222, 1957.
- 5 Ghude, S. D., Vander, R. J., Beig, G., Fadnavis, S., and Polade, S. D.: Satellite derived trends in NO_2 over the major global hotspot regions during the past decade and their inter-comparison, *Environ. Pollut.*, 157, 1873-1878, doi:10.1016/j.envpol.2009.01.013, 2009.
- Goodman, A. L., Bernard, E. T., and Grassian, V. H.: Spectroscopic study of nitric acid and water adsorption on oxide particles: Enhanced nitric acid uptake kinetics in the presence of adsorbed water, *J. Phys. Chem. A*, 105, 6443-6457, doi:10.1021/jp003722l, 2001.
- 10 Goodman, A. L., Underwood, G. M., and Grassian, V. H.: A laboratory study of the heterogeneous reaction of nitric acid on calcium carbonate particles, *J. Geophys. Res.*, 105, 29053-29064, doi:10.1029/2000jd900396, 2000.
- Goodman, A. L., Underwood, G. M., and Grassian, V. H.: Heterogeneous reaction of NO_2 : characterization of gas-phase and adsorbed products from the reaction, $2\text{NO}_2(\text{g}) + \text{H}_2\text{O}(\text{a}) \rightarrow \text{HONO}(\text{g}) + \text{HNO}_3(\text{a})$ on hydrated silica particles, *J. Phys. Chem.*, 103, 7217-7223, doi:10.1021/jp9910688, 1999.
- 15 Guan, C., Li, X., Luo, Y., and Huang, Z.: Heterogeneous reaction of NO_2 on $\alpha\text{-Al}_2\text{O}_3$ in the dark and simulated sunlight, *J. Phys. Chem. A*, 118, 6999-7006, doi:10.1021/jp503017k, 2014.
- 20 Guo, S., Hu, M., Zamora, M. L., Peng, J. F., Shang, D. J., Zheng, J., Du, Z. F., Wu, Z. J., Shao, M., Zeng, L. M., Molina, M. J., and Zhang, R. Y.: Elucidating severe urban haze formation in China, *Proc. Natl. Acad. Sci. U. S. A.*, 111, 17373-17378, doi:10.1073/pnas.1419604111, 2014.
- 25 Huang, K., Zhang, X., and Lin, Y.: The “APEC Blue” phenomenon: Regional emission control effects observed from space, *Atmos. Res.*, 164, 65-75, doi:10.1016/j.atmosres.2015.04.018, 2015.
- Huang, R. J., Zhang, Y., Bozzetti, C., Ho, K. F., Cao, J. J., Han, Y., Daellenbach, K. R., Slowik, J. G., Platt, S. M., Canonaco, F., Zotter, P., Wolf, R., Pieber, S. M., Bruns, E. A.,



- Crippa, M., Ciarelli, G., Piazzalunga, A., Schwikowski, M., Abbaszade, G., Schnelle-Kreis, J., Zimmermann, R., An, Z., Szidat, S., Baltensperger, U., ElHaddad, I., and Prevot, A. S. H.: High secondary aerosol contribution to particulate pollution during haze events in China, *Nature*, 514, 218-222, doi:10.1038/nature13774, 2014.
- 5 Irie, H., Sudo, K., Akimoto, H., Richter, A., Burrows, J. P., Wagner, T., Wenig, M., Beirle, S., Kondo, Y., Sinyakov, V. P., and Goutail, F.: Evaluation of long-term tropospheric NO₂ data obtained by GOME over East Asia in 1996-2002, *Geophys. Res. Lett.*, 32, doi:10.1029/2005gl022770, 2005.
- Jaegle, L., Jacob, D. J., Brune, W. H., Tan, D., Faloona, I. C., Weinheimer, A. J., Ridley, B. A.,
 10 Campos, T. L., and Sachse, G. W.: Sources of HO_x and production of ozone in the upper troposphere over the United States, *Geophys. Res. Lett.*, 25, 1709-1712, doi:10.1029/98gl00041, 1998.
- Jenkin, M. E., Cox, R. A., and Williams, D. J.: Laboratory studies of the kinetics of formation of nitrous-acid from the thermal-reaction of nitrogen-dioxide and water-vapor, *Atmos.*
 15 *Environ.*, 22, 487-498, doi:10.1016/0004-6981(88)90194-1, 1988.
- Jentsch, P. V., Bolanz, R. M., Ciobota, V., Kampe, B., Roesch, P., Majzlan, J., and Popp, J.: Raman spectroscopic study of calcium mixed salts of atmospheric importance, *Vib. Spectros.*, 61, 206-213, doi:10.1016/j.vibspec.2012.03.007, 2012.
- Johnson, E. R., Sciegienka, J., Carlos-Cuellar, S., and Grassian, V. H.: Heterogeneous uptake
 20 of gaseous nitric acid on dolomite CaMg(CO₃)₂ and calcite CaCO₃ particles: A knudsen cell study using multiple, single, and fractional particle layers, *J. Phys. Chem. A*, 109, 6901-6911, doi:10.1021/jp0516285, 2005.
- Kong, L. D., Yang, Y., Zhang, S., Zhao, X., Du, H., Fu, H., Zhang, S., Cheng, T., Yang, X., Chen, J., Wu, D., Shen, J., Hong, S., and Jiao, L.: Observations of linear dependence
 25 between sulfate and nitrate in atmospheric particles, *J. Geophys. Res.-Atmos.*, 119, 341-361, doi:10.1002/2013jd020222, 2014a.
- Kong, L. D., Zhao, X., Sun, Z. Y., Yang, Y. W., Fu, H. B., Zhang, S. C., Cheng, T. T., Yang, X., Wang, L., and Chen, J. M.: The effects of nitrate on the heterogeneous uptake of sulfur dioxide on hematite, *Atmos. Chem. Phys.*, 14, 9451-9467, doi:10.5194/acp-14-9451-2014,



- 2014b.
- Korhonen, H., Napari, I., Timmreck, C., Vehkamäki, H., Pirjola, L., Lehtinen, K. E. J., Lauri, A., and Kulmala, M.: Heterogeneous nucleation as a potential sulphate-coating mechanism of atmospheric mineral dust particles and implications of coated dust on new particle formation, *J. Geophys. Res.-Atmos.*, 108, doi:10.1029/2003jd003553, 2003.
- 5 Kulmala, M.: China's choking cocktail, *Nature*, 526, 497-499, 2015.
- Kuriyavar, S. I., Vetrivel, R., Hegde, S. G., Ramaswamy, A. V., Chakrabarty, D., and Mahapatra, S.: Insights into the formation of hydroxyl ions in calcium carbonate: temperature dependent FTIR and molecular modelling studies, *J. Mater. Chem.*, 10, 1835-1840, doi:10.1039/b001837f, 2000.
- 10 Laskin, A., Iedema, M. J., Ichkovich, A., Graber, E. R., Taraniuk, I., and Rudich, Y.: Direct observation of completely processed calcium carbonate dust particles, *Faraday Discuss.*, 130, 453-468, doi:10.1039/b417366j, 2005.
- Levin, Z., Ganor, E., and Gladstein, V.: The effects of desert particles coated with sulfate on rain formation in the eastern Mediterranean, *J. App. Meteorol.*, 35, 1511-1523, doi:10.1175/1520-0450(1996)035<1511:teodpc>2.0.co;2, 1996.
- 15 Li, H. J., Zhu, T., Zhao, D. F., Zhang, Z. F., and Chen, Z. M. : Kinetics and mechanisms of heterogeneous reaction of NO₂ on CaCO₃ surfaces under dry and wet conditions, *Atmos. Chem. Phys.*, 10, 463-474, 2010.
- 20 Li, L., Chen, Z. M., Zhang, Y. H., Zhu, T., Li, S., Li, H. J., Zhu, L. H., and Xu, B. Y.: Heterogeneous oxidation of sulfur dioxide by ozone on the surface of sodium chloride and its mixtures with other components, *J. Geophys. Res.-Atmos.*, 112, doi:10.1029/2006jd008207, 2007.
- Li, L., Chen, Z. M., Zhang, Y. H., Zhu, T., Li, J. L., and Ding, J.: Kinetics and mechanism of heterogeneous oxidation of sulfur dioxide by ozone on surface of calcium carbonate, *Atmos. Chem. Phys.*, 6, 2453-2464, 2006.
- 25 Li, W. J., Shao, L. Y.: Observation of nitrate coatings on atmospheric mineral dust particles, *Atmos. Chem. Phys.*, 9, 1863-1871, 2009.
- Li, X., Maring, H., Savoie, D., Voss, K., and Prospero, J. M.: Dominance of mineral dust in



- aerosol light-scattering in the North Atlantic trade winds, *Nature*, 380, 416-419, doi:10.1038/380416a0, 1996.
- Lightstone, J. M., Onasch, T. B., Imre, D., and Oatis, S.: Deliquescence, efflorescence, and water activity in ammonium nitrate and mixed ammonium nitrate/succinic acid microparticles, *J. Phys. Chem. A*, 104, 9337-9346, doi:10.1021/jp002137h, 2000.
- 5 Liu, Y. C., Han, C., Ma, J. Z., Bao, X. Z., and He, H.: Influence of relative humidity on heterogeneous kinetics of NO₂ on kaolin and hematite, *Phys. Chem. Chem. Phys.*, 17, 19424-19431, doi:10.1039/c5cp02223a, 2015.
- Liu, Y., Wang, A., Freeman, J. J.: Raman, Mir, and NIR spectroscopic study of calcium sulfates: gypsum, bassanite, and anhydrite, 40th Lunar and Planetary Science Conference, 2009.
- 10 Liu, Y. J., Zhu, T., Zhao, D. F., and Zhang, Z. F.: Investigation of the hygroscopic properties of Ca(NO₃)₂ and internally mixed Ca(NO₃)₂/CaCO₃ particles by micro-Raman spectrometry, *Atmos. Chem. Phys.*, 8, 7205-7215, 2008.
- 15 Ma, Q. X., He, H., Liu, Y. C., Liu, C., and Grassian, V. H.: Heterogeneous and multiphase formation pathways of gypsum in the atmosphere, *Phys. Chem. Chem. Phys.*, 15, 19196-19204, doi:10.1039/c3cp53424c, 2013.
- Miller, T. M., and Grassian, V. H.: Heterogeneous chemistry of NO₂ on mineral oxide particles: Spectroscopic evidence for oxide-coordinated and water-solvated surface nitrate, 20 *Geophys. Res. Lett.*, 25, 3835-3838, doi:10.1029/1998gl900011, 1998.
- Mori, I., Nishikawa, M., and Iwasaka, Y.: Chemical reaction during the coagulation of ammonium sulphate and mineral particles in the atmosphere, *Sci. Tot. Environ.*, 224, 87-91, doi:10.1016/s0048-9697(98)00323-4, 1998.
- Mori, I., Nishikawa, M., Tanimura, T., and Quan, H.: Change in size distribution and chemical composition of kosa (Asian dust) aerosol during long-range transport, *Atmos. Environ.*, 37, 4253-4263, doi:10.1016/s1352-2310(03)00535-1, 2003.
- 25 Pathak, R. K., Wu, W. S., and Wang, T.: Summertime PM_{2.5} ionic species in four major cities of China: nitrate formation in an ammonia-deficient atmosphere, *Atmos. Chem. Phys.*, 9, 1711-1722, 2009



- Possanzini, M., De Santis, F., and Di Palo, V.: Measurements of nitric acid and ammonium salts in lower Bavaria, *Atmos. Environ.*, 33, 3597-3602, doi:10.1016/s1352-2310(99)00096-5, 1999.
- Prasad, P. S. R., Krishna Chaitanya, V., Shiva Prasad, K., and Narayana Rao, D.: Direct
 5 formation of the γ -CaSO₄ phase in dehydration process of gypsum: In situ FTIR study, *Am. Mineral.*, 90, 672-678, doi:10.2138/am.2005.1742, 2005.
- Prince, A. P., Grassian, V. H., Kleiber, P., and Young, M. A.: Heterogeneous conversion of calcite aerosol by nitric acid, *Phys. Chem. Chem. Phys.*, 9, 622-634, doi:10.1039/b613913b, 2007.
- 10 Quan, J., Zhang, X., Zhang, Q., Guo, J., and Vogt, R. D.: Importance of sulfate emission to sulfur deposition at urban and rural sites in China, *Atmos. Res.*, 89, 283-288, doi:10.1016/j.atmosres.2008.02.015, 2008.
- Querol, X., Alastuey, A., Puigercus, J. A., Mantilla, E., Ruiz, C. R., Lopez-Soler, A., Plana, F., and Juan, R.: Seasonal evolution of suspended particles around a large coal-fired power
 15 station: Chemical characterization, *Atmos. Environ.*, 32, 719-731, doi:10.1016/s1352-2310(97)00340-3, 1998.
- Richter, A., Burrows, J. P., Nuss, H., Granier, C., and Niemeier, U.: Increase in tropospheric nitrogen dioxide over China observed from space, *Nature*, 437, 129-132, doi:10.1038/nature04092, 2005.
- 20 Rubasinghege, G., and Grassian, V. H.: Role(s) of adsorbed water in the surface chemistry of environmental interfaces, *Chem. Rev.*, 49, 3071-3094, doi:10.1039/c3cc38872g, 2013.
- Schlenker, J. C., Malinowski, A., Martin, S. T., Hung, H. M., and Rudich, Y.: Crystals formed at 293 K by aqueous sulfate-nitrate-ammonium-proton aerosol particles, *J. Phys. Chem. A*, 108, 9375-9383, doi:10.1021/jp047836z, 2004.
- 25 Sheel, V., Lal, S., Richter, A., and Burrows, J. P.: Comparison of satellite observed tropospheric NO₂ over India with model simulations, *Atmos. Environ.*, 44, 3314-3321, doi:10.1016/j.atmosenv.2010.05.043, 2010.
- Shi, C., Fernando, H. J. S., Wang, Z. F., An, X. Q., and Wu, Q. Z.: Tropospheric NO₂ columns over East Central China: Comparisons between SCIAMACHY measurements and nested



- CMAQ simulations, Atmos. Environ., 42, 7165-7173, doi:10.1016/j.atmosenv.2008.05.046, 2008.
- Sullivan, R. C., Guazzotti, S. A., Sodeman, D. A., and Prather, K. A.: Direct observations of the atmospheric processing of Asian mineral dust, Atmos. Chem. Phys., 7, 1213–1236, 2007.
- Svensson, R., Ljungstrom, E., and Lindqvist, O.: Kinetics of the reaction between nitrogen-dioxide and water-vapor, Atmos. Environ., 21, 1529-1539, doi:10.1016/0004-6981(87)90315-5, 1987.
- Tang, I. N., and Fung, K. H.: Hydration and Raman scattering studies of levitated microparticles: Ba(NO₃)₂, Sr(NO₃)₂, and Ca(NO₃)₂, J. Chem. Phys., 106, 1653-1660, doi:10.1063/1.473318, 1997.
- Tegen, I., Lacis, A. A., and Fung, I.: The influence on climate forcing of mineral aerosols from disturbed soils, Nature, 380, 419-422, doi:10.1038/380419a0, 1996.
- Tong, S. R., Wu, L. Y., Ge, M. F., Wang, W. G., and Pu, Z. F.: Heterogeneous chemistry of monocarboxylic acids on α -Al₂O₃ at different relative humidities, Atmos. Chem. Phys., 10, 7561-7574, doi:10.5194/acp-10-7561-2010, 2010.
- Ullerstam, M., Vogt, R., Langer, S., and Ljungstrom, E.: The kinetics and mechanism of SO₂ oxidation by O₃ on mineral dust, Phys. Chem. Chem. Phys., 4, 4694-4699, doi:10.1039/b203529b, 2002.
- Underwood, G. M., Li, P., Usher, C. R., and Grassian, V. H.: Determining accurate kinetic parameters of potentially important heterogeneous atmospheric reactions on solid particle surfaces with a Knudsen Cell Reactor, J. Phys. Chem. A, 104, 819-829, doi:10.1021/jp9930292, 1999a.
- Underwood, G. M., Miller, T. M., and Grassian, V. H.: Transmission FT-IR and Knudsen Cell study of the heterogeneous reactivity of gaseous nitrogen dioxide on mineral oxide particles, J. Phys. Chem. A, 103, 6184-6190, doi:10.1021/jp991586i, 1999b.
- Usher, C. R., Michel, A. E., and Grassian, V. H.: Reactions on mineral dust, Chem. Rev., 103, 4883-4939, doi:10.1021/cr020657y, 2003.
- Vogt, R., and Finlaysonpitts, B. J.: A Diffuse Reflectance Infrared Fourier-Transform



- Spectroscopic (DRIFTS) study of the surface-reaction of NaCl with gaseous NO₂ and HNO₃, *J. Phys. Chem.*, 98, 3747-3755, doi:10.1021/j100065a033, 1994.
- Volz, A., and Kley, D.: Evaluation of the montsouris series of ozone measurements made in the 19th-century, *Nature*, 332, 240-242, doi:10.1038/332240a0, 1988.
- 5 Wang, Y., Zhang, Q. Q., He, K., Zhang, Q., and Chai, L.: Sulfate-nitrate-ammonium aerosols over China: response to 2000-2015 emission changes of sulfur dioxide, nitrogen oxides, and ammonia, *Atmos. Chem. Phys.*, 13, 2635-2652, doi:10.5194/acp-13-2635-2013, 2013.
- Wu, L. Y., Tong, S. R., and Ge, M. F.: Heterogeneous reaction of NO₂ on Al₂O₃: the effect of temperature on the nitrite and nitrate formation, *J. Phys. Chem. A*, 117, 4937-4944,
10 doi:10.1021/jp402773c, 2013.
- Yang, F., Tan, J., Zhao, Q., Du, Z., He, K., Ma, Y., Duan, F., Chen, G., and Zhao, Q.: Characteristics of PM_{2.5} speciation in representative megacities and across China, *Atmos. Chem. Phys.*, 11, 5207-5219, doi:10.5194/acp-11-5207-2011, 2011.
- Zamaraev, K. I., Khramov, M. I., and Parmon, V. N.: Possible impact of heterogeneous
15 photocatalysis on the global chemistry of the earths atmosphere, *Cat. Rev.-Sci. Eng.*, 36, 617-644, doi:10.1080/01614949408013930, 1994.
- Zhang, D. Z., Shi, G. Y., Iwasaka, Y., and Hu, M.: Mixture of sulfate and nitrate in coastal atmospheric aerosols: individual particle studies in Qingdao (36 degrees 04 ' N, 120 degrees 21 ' E), China, *Atmos. Environ.*, 34, 2669-2679, doi:10.1016/s1352-2310(00)000
20 78-9, 2000.
- Zhang, Q., Streets, D. G., He, K., Wang, Y., Richter, A., Burrows, J. P., Uno, I., Jang, C. J., Chen, D., Yao, Z., and Lei, Y.: NO_x emission trends for China, 1995-2004: The view from the ground and the view from space, *J. Geophys. Res.-Atmos.*, 112, doi:10.1029/2007jd008684, 2007.
- 25 Zhang, R. Y., Wang, G. H., Guo, S., Zamora, M. L., Ying, Q., Lin, Y., Wang, W. G., Hu, M., and Wang, Y.: Formation of urban fine particulate matter, *Chem. Rev.*, 115, 3803-3855, doi:10.1021/acs.chemrev.5b00067, 2015.
- Zhao, Y., Chen, Z. M., Shen, X. L., and Huang, D.: Heterogeneous reactions of gaseous hydrogen peroxide on pristine and acidic gas-processed calcium carbonate particles:



Effects of relative humidity and surface coverage of coating, Atmos. Environ., 67, 63-72,
doi:10.1016/j.atmosenv.2012.10.055, 2013.

Zheng, G. J., Duan, F. K., Su, H., Ma, Y. L., Cheng, Y., Zheng, B., Zhang, Q., Huang, T.,
Kimoto, T., Chang, D., Pöschl, U., Cheng, Y. F., and He, K. B.: Exploring the severe winter
5 haze in Beijing: the impact of synoptic weather, regional transport and heterogeneous
reactions, Atmos. Chem. Phys., 15, 2969-2983, doi:10.5194/acp-15-2969-2015, 2015.



Table 1. Assignments of IR vibration frequencies of surface adsorbed species formed on CaCO_3 particle surfaces and $\text{CaCO}_3\text{-(NH}_4)_2\text{SO}_4$ mixtures

Samples	Stretch mode	ν_1 (cm^{-1})	ν_2 (cm^{-1})	ν_3 (cm^{-1})	ν_4 (cm^{-1})	Stretch mode
$\text{Ca(NO}_3)_2$	NO_3^-	1043	816	1300, 1330,	748	
$^a\text{NH}_4\text{NO}_3$	NO_3^-	1050	830	1333, 1365		NH_4^+ 1426, 1451
$\text{CaSO}_4 \cdot 0.5\text{H}_2\text{O}$	SO_4^{2-}	1008		1096, 1116, 1155, 1168		H_2O 1620, 3553, 3605
$^b\text{CaSO}_4 \cdot 0.5\text{H}_2\text{O}$	SO_4^{2-}	1008		1096, 1116, 1153, 1168	601, 660	H_2O 1620, 3550, 3610
$\text{CaSO}_4 \cdot 2\text{H}_2\text{O}$	SO_4^{2-}	1003		1117, 1145, 1167		H_2O 1620, 1685, 3400, 3545
$^c\text{CaSO}_4 \cdot 2\text{H}_2\text{O}$	SO_4^{2-}	1005		1117, 1145, 1167	602, 669	H_2O 1621, 1685, 3405, 3495, 3547
$(\text{NH}_4)_2\text{Ca(SO}_4)_2 \cdot \text{H}_2\text{O}$	SO_4^{2-}	981, 998		1131, 1177		H_2O 2860, 3064, 3192
$^d(\text{NH}_4)_2\text{Ca(SO}_4)_2 \cdot \text{H}_2\text{O}$	SO_4^{2-}	981, 998		1108, 1131, 1177	602, 614, 646, 656	H_2O 2857, 2922, 3125, 3192

^a from Schlenker et al. (2004). ^{b,c} from Prasad et al. (2005). ^d from Jentzsch et al. (2012)



Table 2. Initial uptake coefficients calculated using BET surface area and geometric surface area for NO₂ on CaCO₃ particle surfaces and CaCO₃-(NH₄)₂SO₄ mixtures at various RHs.

(NH ₄) ₂ SO ₄ (wt%)	dry condition		40% RH		60% RH		85% RH	
	γ_{BET} ($\times 10^{-9}$)	γ_{geo} ($\times 10^{-6}$)	γ_{BET} ($\times 10^{-9}$)	γ_{geo} ($\times 10^{-6}$)	γ_{BET} ($\times 10^{-9}$)	γ_{geo} ($\times 10^{-6}$)	γ_{BET} ($\times 10^{-9}$)	γ_{geo} ($\times 10^{-6}$)
0	3.34±0.14	10.4±0.44	2.04±0.07	6.36±0.22	2.23±0.22	6.94±0.69	2.28±0.17	7.10±0.53
10	3.19±0.21	9.83±0.65	2.06±0.21	6.34±0.45	2.25±0.14	6.91±0.43	2.13±0.41	6.56±1.26
20	3.77±0.24	9.54±0.61	2.51±0.34	6.28±0.86	2.74±0.42	6.87±1.06	2.00±0.21	5.63±0.53
40	5.34±0.17	9.25±0.29	3.50±0.42	6.07±0.72	3.67±0.48	6.36±0.83	3.15±0.28	5.46±0.49
57	6.82±0.33	8.38±0.41	4.70±0.51	5.78±0.63	4.47±0.26	5.49±0.32	4.15±0.53	5.10±0.65
75	7.74±0.94	6.94±0.84	6.12±0.37	5.49±0.23	5.80±0.53	5.20±0.48	4.26±0.31	3.82±0.28
87	9.04±0.73	5.78±0.46	7.68±0.50	4.92±0.32	7.22±0.63	4.63±0.40	4.83±0.46	3.10±0.19
93	14.4±1.07	4.90±0.36	13.6±0.93	4.63±0.32	12.7±0.81	4.34±0.28	7.48±0.82	2.55±0.28

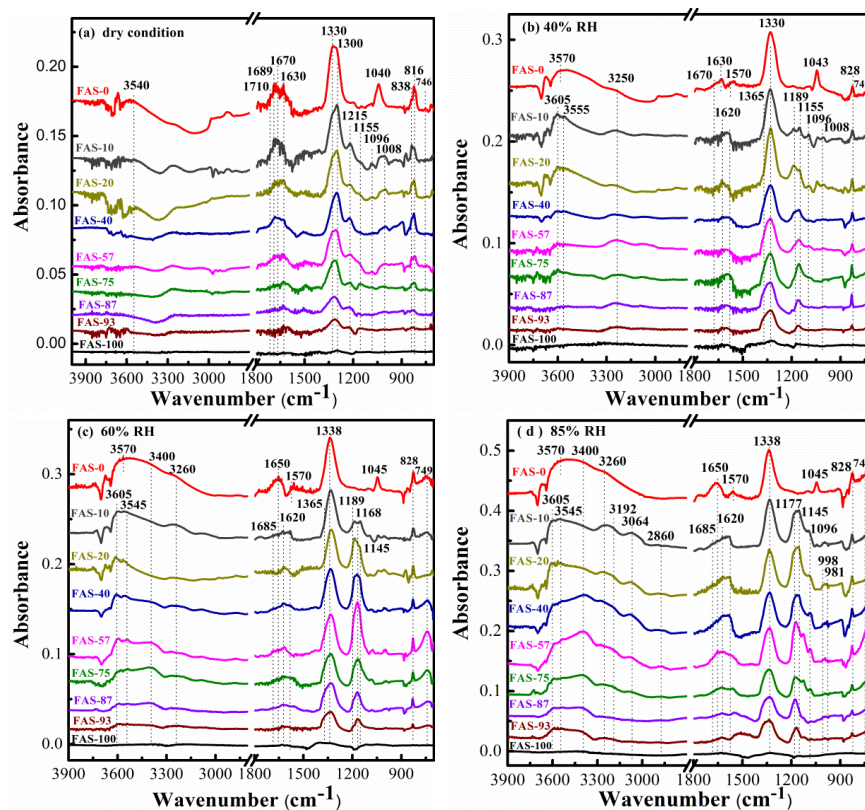


Figure 1. DRIFTS spectra of CaCO_3 particles (FAS-0), $\text{CaCO}_3\text{-(NH}_4)_2\text{SO}_4$ mixtures (FAS-10 - FAS-93), and $(\text{NH}_4)_2\text{SO}_4$ particles (FAS-100) after reaction with NO_2 at (a) dry condition, (b) 40% RH, (c) 60% RH, (d) 85% RH for 120 min. NO_2 concentration was 2.6×10^{15} molecule cm^{-3} .

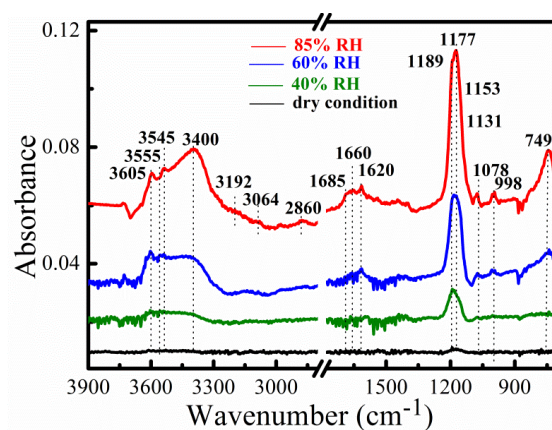


Figure 2. In situ DRIFTS spectra of surface products when the mixture of FAS-57 were exposed to nitrogen at dry condition (black), 40% RH(green), 60% RH(blue) and 85% RH (red) for 120 min.

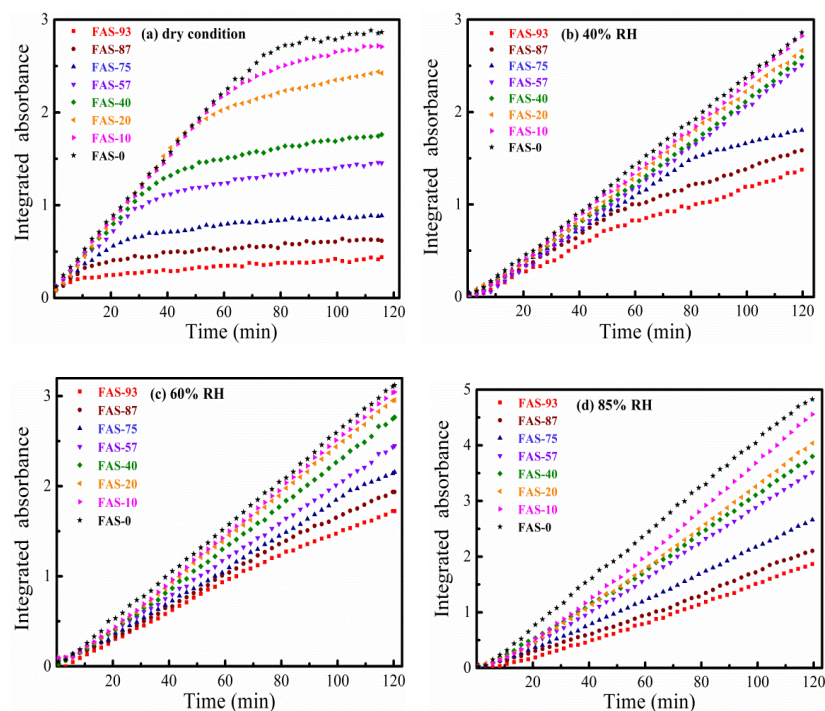


Figure 3. The integrated absorbance of the peak area between 1390 and 1250 cm⁻¹ for nitrate on pure CaCO₃ particle surfaces (FAS-0), and CaCO₃-(NH₄)₂SO₄ mixtures (FAS-10 - FAS-93) at (a) dry condition, (b) 40% RH, (c) 60% RH, and (d) 85% RH. The NO₂ concentration was 2.6×10¹⁵ molecule cm⁻³.

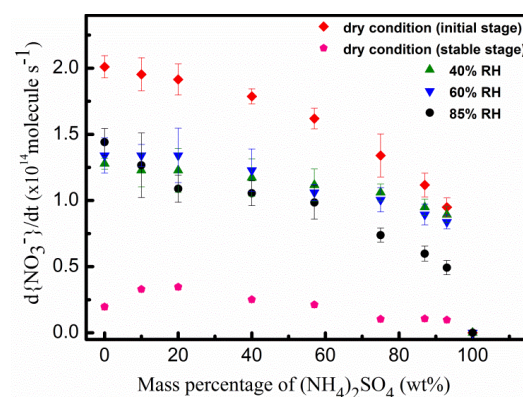


Figure 4. Initial nitrate formation rates at dry condition (rhombus), 40% RH (triangle), 60% RH (fall triangle), 85% RH (roundness) and stable nitrate formation rate (pentagon) under dry condition versus the mass percentage of $(\text{NH}_4)_2\text{SO}_4$ in the mixtures. The data points and the error bars are the average value and the standard deviation of three duplicate experiments.

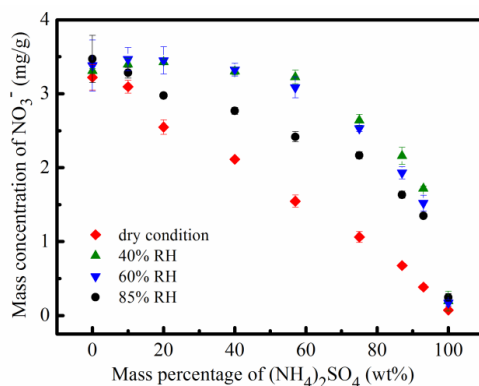


Figure 5. The mass concentration of NO_3^- for CaCO_3 particles and the CaCO_3 - $(\text{NH}_4)_2\text{SO}_4$ mixtures after reacted with NO_2 for 120 min as a function of the mass percentage of $(\text{NH}_4)_2\text{SO}_4$ in the mixtures. The data points and the error bars are the average value and the standard deviation of three duplicate experiments.

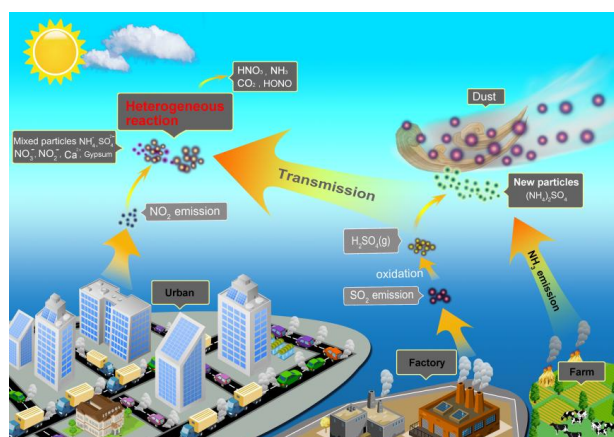


Figure 6. Schematic illustrating the possible heterogeneous processes of NO₂ with CaCO₃-(NH₄)₂SO₄ mixtures and the possible atmospheric implications.